Full Paper

Propellants, Explosives, Pyrotechnics

DOI: 10.1002/prep.201700171

Study of the Elaboration of HMX and HMX Composites by the Spray Flash Evaporation Process

Vincent Pichot,*[a] Aymeric Seve,[a] Jean-Edouard Berthe,[a] Fabien Schnell,[a] and Denis Spitzer[a]

Abstract: The Spray Flash Evaporation (SFE) process invented and developed at the NS3E laboratory allows obtaining different nanosized explosives (TNT, RDX, CL-20…). This process is based on the very fast evaporation of the solvent due to the drastic modification of pressure and temperature leading to the crystallization of the molecules present in solution into nanometric or submicrometric particles. Here, we show the possibility to prepare pure HMX (Octahydro-1,3,5,7-tetranitro-1,3,5,7-tetrazocine) or HMX based composites at the nanoscale using this process. This study mainly focuses on the size, morphology and crystallographic phases obtained for HMX and HMX/TNT composites depending on the experimental conditions (temperature, pressure, solution concentration…) used during the elaboration. For this purpose, the results obtained from scanning electron microscopy, X-ray diffraction and Raman spectroscopy are discussed.

Keywords: HMX · TNT · nanosized · Spray Flash Evaporation · composites

1 Introduction

Many techniques can be used to prepare nanoexplosive materials. Spray Flash Evaporation (SFE) process is a very versatile process as it allows synthesizing pure products, mixtures, nanosized cocrystals or core-shell structures [1–4]. Anti-solvent method, Rapid Expansion of Supercritical Solutions (RESS) and Physical Vapor Deposition (PVD) techniques [5–7] are also among the most successful techniques.

Concerning HMX (Octahydro-1,3,5,7-tetranitro-1,3,5,7-tetrazocine), antisolvent, milling, grinding, spray drying and Spray Flash Evaporation succeeded in obtaining nanoparticles [8–13]. Careful studies of the morphologies, the structure and the size of the particles were conducted. Kumar and coworkers were able to synthesized nano – submicron sized RDX and HMX particles using antisolvent method with various solvents such as ethyl acetate, dimethyl sulfoxide, methanol, ethanol… [8]. Liu, Wang and Koch used grinding and milling to decrease the size of HMX micronsized particles down to submicrometer particles around 160–270 nm [9–11]. Spray drying experiments performed by Qiu and coworkers allowed obtaining 100 nm particles of HMX trapped in granules of polymer [12]. Finally, Risse et al. have obtained HMX particles with sizes down to 120 nm using the SFE process [13]. Among these techniques, milling and grinding are not suitable. The used beads transferring a lot of energy to the explosive materials can become hazardous. Spray drying may be interesting but it usually allows to synthesize micron sized particles and in the study of Qiu et al. nanosized HMX particles could be produced but with a polymer. The antisolvent and the SFE process seem to be the most promising techniques to finely control the size, morphology and structure of explosives.

HMX exhibits different polymorph structures which can crystallize in different systems. Miller and Garroway wrote a review on the crystal structures of various explosives and address the case of HMX [14]. Four different HMX phases are reported: β-HMX, α-HMX, γ-HMX and δ-HMX, their densities are quite different 1.90, 1.84, 1.76 and 1.80 g.cm^{-3} respectively. Nevertheless, it is pointed out that the γ-HMX phase is not a true polymorph of HMX but rather a hydrate 2 $C_4H_8N_8O_8$—0.5 H_2O. Soni and coworkers also presented the polymorphism of HMX and considered the phase transformation between the different phases [15].

A previous study has shown that the use of nanostructured octolite for the synthesis of detonation nanodiamonds leads to very small nanodiamonds with even a narrower size distribution [16]. This result can be linked to different parameters such as the density, the structure, the size of the nanoparticles in the explosive charge. For this reason, a whole study of the HMX and HMX composites was undertaken in order to better understand the influence of the characteristics of the explosive phases used in the detonation experiment. In this paper we propose to deal with the characteristics of the synthesized HMX and HMX based nanocomposites in order to try to control and to understand the structure, the size and the morphology of the particles.

[a] *V. Pichot, A. Seve, J.-E. Berthe, F. Schnell, D. Spitzer*
NS3E "Nanomatériaux pour les Systèmes Sous Sollicitations Extrêmes" UMR 3208 ISL/CNRS/UNISTRA)
French German research insitute of Saint-Louis (ISL)
5 rue du général Cassagnou, 68301, Saint-Louis, France
**e-mail: vincent.pichot@isl.eu*

2 Experimental Section

2.1 Materials

Pure HMX (Dyno, CAS: 2691-41-0) and TNT (Trinitrotoluene, Eurenco, CAS: 118-96-7) were used for this study. Solutions of HMX/TNT with different ratios (100/0, 80/20, 60/40, 40/60 and 20/80 wt%) were prepared in acetone purchased from Sigma Aldrich (Chromasolv® for HPLC $\geq$ 99.8 %). The concentrations were of 2 wt% in pure HMX solution and 4 wt% in HMX/TNT solutions. The HMX used in this study was given by the provider to have a purity of 98.8 % containing 1.2 % of RDX and no acetone insoluble material. Nuclear Magnetic Resonance (NMR) was used at our laboratory to confirm these values. X-Ray Diffraction (XRD) experiment performed on this HMX revealed a product constituted entirely of β-HMX.

2.2 HMX, HMX Based Composites Elaboration

The preparation of the nanosized products was achieved by SFE which was invented and developed at the NS3E laboratory. The principle of this process has already been reported in detail several times [1–3] Briefly, it consists in vaporizing heated and pressurized solutions containing the product to crystallize through a hollow cone nozzle into an atomization chamber which is under vacuum (few hPa). The solutions are initially pressurized at 4 MPa in container. The pressure and the temperature were maintained constant in the nozzle during the whole experiment. The rapid drop of pressure and temperature occurring at the end of the nozzle leads to a very fast crystallization of the product. The nanoparticles are then recovered in filters (room temperature). Concerning the pure HMX preparation, the pressure and temperature used in two samples were 4 MPa and 110 °C (sample 1) and 4 MPa and 160 °C (sample 2) respectively. The experimental conditions used to produce the HMX/TNT composites (20/80, 40/60, 60/40 and 80/20 wt %) were 4 MPa and 160 °C for the pressure and temperature respectively.

2.3 Characterizations

Morphologies of synthesized products were imaged by a Philips XL-30 FEG Scanning Electronic Microscope (SEM).

The size distributions were obtained from measuring the particle sizes of more than 250 particles in each sample. The distributions were fitted by lognormal curves.

X-ray diffraction (XRD) was performed on a Bruker D8 Advance powder diffraction spectrometer with Cu Kα1 radiation ($\lambda = 0.154$ nm).

Raman spectra were recorded using invia Renishaw spectrometer with a 514 nm laser including an edge filter and a grating of 1800 l/mm. Data were collected thanks to a CCD camera.

The 1H Nuclear Magnetic Resonance spectra were performed on a Varian MR 400 with 400 MHz frequency and a magnetic field of 7.6 Tesla.

3 Results and Discussion

3.1 Pure HMX

The size and the morphology of the nano HMX (n-HMX) particles obtained by SFE process has been analyzed by Scanning Electron Microscopy (SEM). Figure 1 shows some micrographs obtained from sample 1 and 2. While sample 1 exhibits micrometric rod shaped particles, sample 2 reveals different types of morphology with spherical shaped particles and not well defined or faceted particles with sizes below 500 nm. The size distributions were obtained from measuring the particle sizes from the SEM micrographs for both samples. The rods of sample 1 have a length around 6 μm and a width around 1 μm, on the other hand the mean diameter of the sample 2 particles is found to be 250 nm.

These products were analyzed by NMR after being dissolved in deuterated aceton. They both exhibit the bands of HMX (f1: 5.99 ppm) and RDX (f1: 6.06 ppm). This allow determining a HMX and RDX contents of 99 wt% and 1 wt% respectively. These results are in good agreement with the purity measured on the HMX sample prior to put them in the SFE process. Structural investigations were conducted by X-Ray Diffraction (XRD) and Raman spectroscopy.

The XRD patterns of the two samples (black lines) reveal mainly a γ-HMX phase in both cases (PDF file n°044-1621). However, small amount of α-HMX (PDF file n°025-1748) can also be detected in sample 1 (Figure 2). These results are different from the one obtained by Risse et al. who found some β-HMX for operating conditions of 6 MPa and 160 °C with the same technique [13]. Depending on the initial pressure and temperature parameters different phases can be obtained using the SFE technique. After a few months the XRD patterns were recorded a second time (grey line) on the same samples and a clear phase transition of the HMX from gamma phase to alpha phase could be observed in sample 1. Concerning sample 2, the majority phase remains the γ-HMX while small diffraction peaks of beta phase (PDF file n°045-1748) could be observed. Figure 3 confirms the XRD results by revealing the α-HMX phase for sample 1 and the γ-HMX phase for the sample 2 after few months of ageing thanks to the Raman spectroscopy. The Raman vibrational frequencies of the different HMX phases can be found in reference [17].

Previous study has evidenced the phase transitions of HMX by Raman spectroscopy depending on the phase and the heating rate conditions when heating under a nitrogen flux the phase transitions [17]. According to their results the

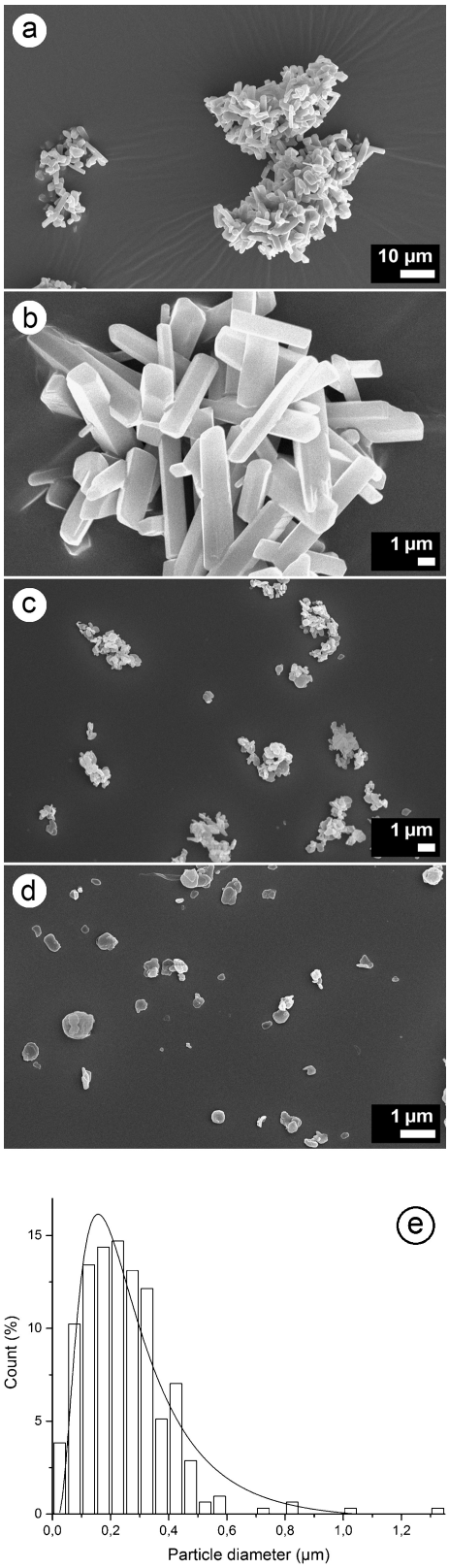

Figure 1. Scanning Electron Microscopy micrographs obtained from sample 1 (a, b) and sample 2 (c, d); size distribution of the particles obtained in the case of a temperature of 160 °C used in the process (e).

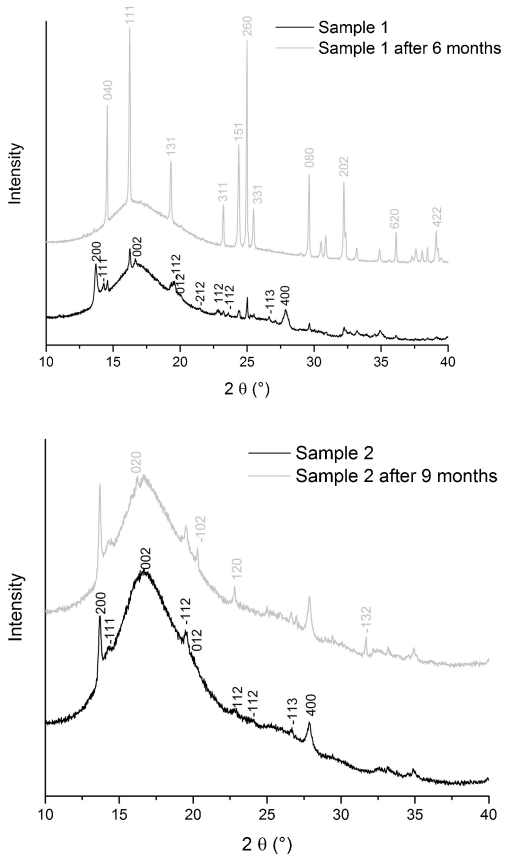

Figure 2. XRD patterns obtained from sample 1 and 2 directly after the elaboration and few months after. Black peak indexation is the one of γ-HMX, grey peak indexations in sample 1 and 2 are for α-HMX and β-HMX respectively. The broad signal from ~13 to ~20° is a result of the amorphous PMMA sample holder that leads to this background.

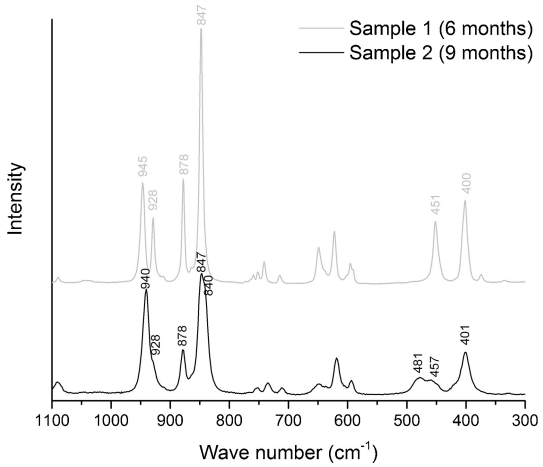

Figure 3. Raman spectra of sample 1 and 2 after months of ageing at room temperature.

transitions were found to be reproducible. Transition of γ-HMX phase to α or β-HMX is obtained at a temperature around 173–183 °C. Moore et al. prepared some submicron sized γ-HMX by antisolvent method and studied the effect of compression on the γ-HMX to β-HMX phase transition [18]. They showed the percentage of phase transition completion depending on the duration and the intensity of the compression. Fractions of γ-HMX could be successfully converted into β-HMX by pressing at 80 MPa during few minutes. Akkbarzade et al. have performed molecular dynamics simulations to calculate the interaction potential energy and sublimation enthalpy of HMX [19]. They found that for all the studied sizes (nanoparticles < 10 nm) the most stable phase is the β-HMX followed by the α-HMX and then the δ-HMX. They also pointed out that the nanoparticles becomes more stable when their size increases. Soni et al. observed a phase transition from γ-HMX to β-HMX when the γ form is heated with water (85 °C during 1 h). The water associated with HMX is removed and it converts to the β form of HMX [15].

In the light of these works, one can infer that the phase transitions of HMX forms does not so easily occur to happen. They often need some heating or compression to occur. However, these transitions are possible. Nevertheless, phase transitions were observed in both samples after a very long time (months). Maybe, the kinetics of transformations of the γ-HMX phase to a more stable form is very slow at room temperature. γ-HMX is a hydrated phase, during this period the water trapped in the γ-HMX phase could have been removed from the crystal leading to a more stable phase.

Small proportions of α-HMX were present in sample 1; this may have helped the transformation of γ-HMX phase into α-HMX. The α-HMX crystals may have served as seeds for the transformation. In the case of the second sample which seems to be free of α-HMX phase maybe some water present near the surface of the crystals phase has evaporated leading to the transition of some parts of the crystals into β-HMX. However, these assumptions would need further experiments and especially a whole specific transition phase study to allow us to conclude properly about the ageing of the products.

One of the very important point to try to understand the phase transition would be to figure out where the water present in the γ-HMX phase comes from. In this study, as received and dried HMX were tested before the elaboration in order to check if the water was coming from the starting material but the same results were obtained. HPLC grade acetone was used as solvent for the solution preparation meaning that water cannot comefrom the solvent. The sample 2 was placed in an oven at 60 °C during two days (after the 9 months at room temperature) in order to try to remove the water present in the γ-HMX phase. No subsequent phase transformation into β-HMX could be observed. These results raise the question about the γ-HMX phase which is found directly after the synthesis. Is it a solvate instead of a hydrate with acetone molecules replacing the water molecule in the HMX structure?

3.2 HMX Composites

The four HMX/TNT composites (20/80, 40/60, 60/40, 80/20) were analyzed by NMR. The different molar and weight ratios are reported in Table 1.

Table 1. Molar and weight ratios measured by NMR in the HMX/TNT composites

HMX/TNT	HMX molar %	HMX wt %	TNT molar %	TNT wt %
20/80	17	21	83	79
40/60	34	41	66	59
60/40	54	61	46	39
80/20	76	81	24	19

The weight ratios strictly correspond to the ones introduced initially in the solutions. The size and morphology of the particles have been analyzed in the four samples. The particles have a round shape or faceted morphology, individual or agglomerated particles can be found (Figure 4). The size of the particles have been measured on hundreds of particles for each sample. The size distributions are given in Figure 4. The mean diameter of the particles are 130, 90, 50 and 145 nm for the octolites 20/80, 40/60, 60/40 and 80/20 respectively.

Concerning these samples, it is difficult to say whether the samples are composed of individual HMX and TNT particles or if there are some core-shell structures as it was evidenced by Tip Enhanced Raman Spectroscopy in the case of TNT/RDX composites [4].

It can be noticed that the size of the particles decreases when the TNT content increases until it reaches 80 wt% for which the diameter of the particles increases again. TNT may play the role of growth inhibitor by surrounding the HMX particles. For low TNT content the size of the particle is getting closer to the size of raw HMX synthesized by SFE and for high TNT content the particles also increase until having the size of TNT particles synthesized by SFE (i.e. few micrometers [20]).

As for sample 2 (pure HMX synthesized at 4 MPa, 160 °C), the XRD patterns reveal a γ phase of the HMX (PDF file n°044-1621). The contribution of orthorhombic TNT phase (Crystallography Open Database n°5000107 from [21]) is also present as in work of Seve et al. [20]. As expected, it can be clearly seen that the signal of TNT is even more pronounced when the TNT content in the samples is more important. On the contrary when the quantity of HMX decrease the intensities of the HMX peaks also decrease (Figure 5). This indicates that independently of the composition, the same crystal structure is always observed.

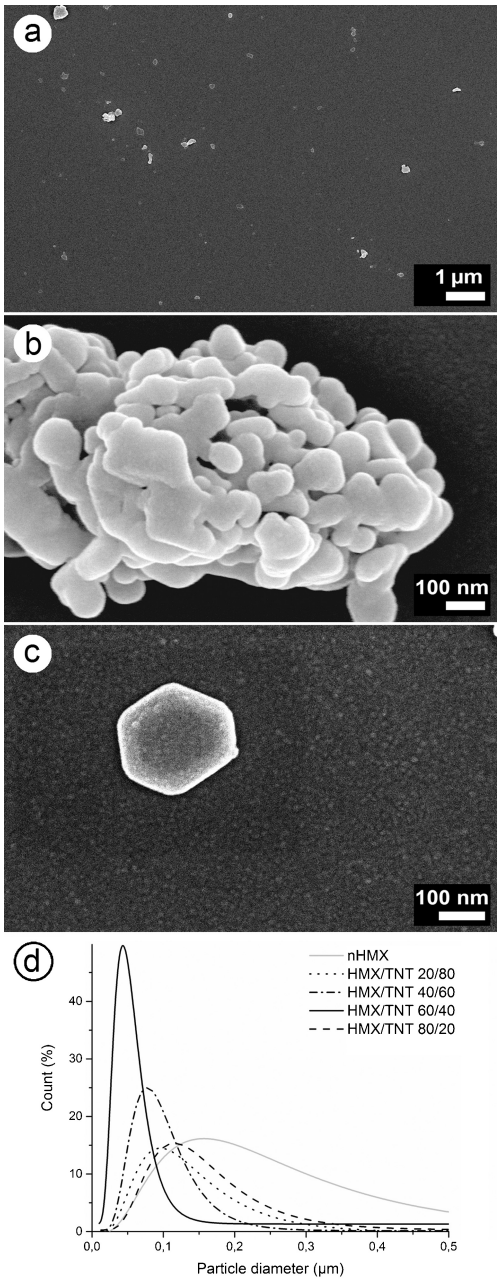

Figure 4. Samples of SEM micrographs obtained from HMX/TNT composites (a–c). Size distribution of the four HMX/TNT composites (d).

The composites were placed in an oven at 60 °C during 2 days in order to see if a phase transition of the γ-HMX phase could occur. No loss of mass due to water evaporation or no apparition of β-HMX diffraction peaks could be observed meaning the good stability of these product conversely to sample 2 for which a small proportion of γ-HMX transformed into β-HMX.

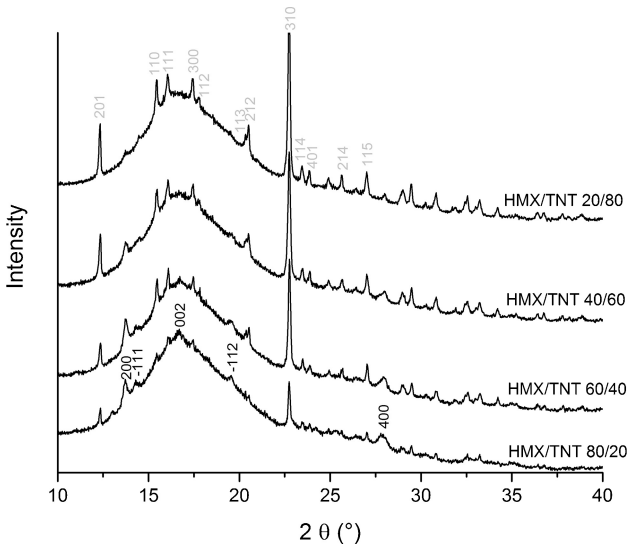

Figure 5. XRD patterns obtained from HMX/TNT composites. The broad signal from ~13 to ~20° is a result of the amorphous PMMA sample holder that leads to this background. Black peak indexation is the one of γ-HMX, grey peak indexation is for TNT.

4 Conclusions

Depending on the initial pressure and temperature parameters, different phases can be obtained by using the SFE technique. A low temperature (110 °C, 4 MPa) allows the elaboration of α-HMX and γ-HMX while a higher temperature with the same pressure (160 °C, 4 MPa) favors the formation of only γ HMX and a higher pressure (160 °C, 6 MPa) leads to the predominance of the β-HMX phase. Further investigations on the pressure and temperature domains of existence of the different phase would be required. Moreover, a temperature of 110 °C leads to the formation of micrometric particles while experiments achieved at higher temperature leads to smaller particles.

The sample synthesized at 110 °C, 4 MPa exhibits a phase transition from γ-HMX to α-HMX probably due to an ageing process and the presence of α-HMX seeds in the sample. The sample containing only γ-HMX is rather stable with only a slight part transforming into β-HMX after a very long time. In composites containing HMX and TNT, the HMX also appears in its γ-HMX phase and no transformation into α or β HMX phases occurred with time or heating at 60 °C. However a complete study with defined conditions of ageing is required to give more informations about the mechanisms and kinetics of the ageing process.

Further experiments using Tip Enhanced Raman Spectroscopy should allow to reveal the arrangement of the HMX and TNT in the sample and to infer the role of TNT as a growth inhibitor for HMX.

This study will be continued by pressing the synthesized products in order to obtain explosive charges used in the synthesis of detonation nanodiamonds.

Acknowledgements

The authors thank K.-T. Han for NMR measurements. This research was funded by the French ANR ASTRID program.

References

[1] B. Risse, D. Spitzer, D.Hassler, F. Schnell, M. Comet, V. Pichot, H. Muhr, Continuous formation of submicron energetic particles by the flash-evaporation technique, *Chemical Engineering Journal* **2012**, *203*, 158-165.

[2] D. Spitzer, B. Risse, F. Schnell, V. Pichot, M. Klaumünzer, M. R. Schaefer, Continuous engineering of nano-cocrystals for medical and energetic applications, *Scientific Reports* **2014**, *4*, 1–6.

[3] F. Pessina, F. Schnell, D. Spitzer, Tunable continuous production of RDX from microns to nanoscale using polymeric additives, *The Chemical Engineering Journal* **2016**, *291*, 12–19.

[4] T. Deckert-Gaudig, V. Pichot, D. Spitzer, V. Deckert, High-resolution Raman Spectroscopy for the Nanostructural Characterization of Explosive Nanodiamond Precursors, *Chemphyschem* **2017**, *18*, 175–178.

[5] B. Huang, M. Cao, F. Nie, H. Huang, C. Hu, Construction and Properties of Structure- and Size-controlled Micro/nano-Energetic Materials, *Defence Technology* **2013**, *9*, 59–79.

[6] V. Stepanov, I. B. Elkina, T. Matsunaga, A. V. Chernyshev, E. N. Chesnokov, X. Zhang, N. L. Lavrik, L. N. Krasnoperov, Production of nanocrystalline RDX by rapid expansion of supercritical solutions, *International Journal of Energetic Materials and Chemical Propulsion* **2007**, *6*, 75–87.

[7] V. Stepanov, Production of nanocrystalline RDX by RESS: Process development and material characterization New Jersey Institute of Technology, **2008**.

[8] R. Kumar, P. F. Siril, P. Soni, Optimized Synthesis of HMX Nanoparticles Using Antisolvent Precipitation Method, *Journal of Energetic Materials* **2015**, *33*, 277–287.

[9] J. Liu, W. Jiang, Q. Yang, J. Song, G. Hao, F. Li, Study of nanonitramine explosives: preparation, sensitivity and application, *Defence Technology* **2014**, *10*, 184–189.

[10] Y. Wang, W. Jiang, X. Song, G. Deng, F. Li, Insensitive HMX (Octahydro-1,3,5,7-tetranitro-1,3,5,7-tetrazocine) Nanocrystals Fabricated by High-Yield, Low-Cost Mechanical Milling, *Central European Journal of Energetic Materials* **2013**, *10*, 277–287.

[11] C. C. Koch, Synthesis of nanostructured materials by mechanical milling: problems and opportunities, *Nanostructured Materials* **1997**, *9*, 13–22.

[12] H. Qiu, V. Stepanov, T. Chou, A. Surapaneni, A. R. Di Stasio, W. Y. Lee, Single-step production and formulation of HMX nanocrystals, *Powder Technology* **2012**, *226*, 235–238.

[13] B. Risse, F. Schnell, D. Spitzer, Synthesis and Desensitization of Nano-β-HMX, *Propellants, Explosives, Pyrotechnics* **2014**, *39*, 397–401.

[14] G. R. Miller, A. N. Garroway, A Review of the Crystal Structures of Common Explosives Part I: RDX, HMX, TNT, PETN, and Tetryl, Naval Research Laboratory, Washington, DC, October 15, **2001**, NRL/MR/6120–01-8585.

[15] P. Soni, C. Sarkar, R. Tewari, T. D. Sharma, HMX Polymorphs: Gamma to Beta Phase Transformation, *Journal of Energetic Materials* **2011**, *29*, 261–279.

[16] V. Pichot, M.Comet, B. Risse, D. Spitzer, Detonation of nanosized explosive: new mechanistic model for nanodiamond formation, *Diamond and related Materials* **2015**, *54*, 59–63.

[17] F. Goetz, T. B. Brill, Laser Raman spectra of alpha-, beta-, gamma-, and delta-octahydro-1,3,5,7-tetranitro-1,3,5,7-tetrazocine and their temperature dependence, *The Journal of Physical Chemistry* **1979**, *83*, 340–346.

[18] D. S. Moore, K. –Y. Lee, S. I. Halgelberg, Submicron-Sized Gamma-HMX: II. Effect of Pressing on Phase Transition Journal of Energetic Materials **2007**, *26*, 70–78.

[19] H. Akkbarzade, G. A. Parsafar, Y. Bayat, Structural stability of nano-sized crystals of HMX: A molecular dynamics simulation study, *Applied Surface Science* **2012**, *258*, 2226–2230.

[20] A. Seve, V. Pichot, F. Schnell, D. Spitzer, Trinitrotoluene Nanostructuring by Spray Flash Evaporation Process, *Propellants, Explosives, Pyrotechnics* **2017**, DOI: 10.1002/prep.201700024.

[21] W. R. Carper, L. P. Davis, Molecular structure of 2,4,6-trinitrotoluene, *The Journal of Physical Chemistry* **1982**, *86*, 459–462.

Received: June 27, 2017
Revised: September 11, 2017
Published online: November 8, 2017

